

Early Lane Change Prediction for Automated Driving Systems Using Multi-Task Attention-based Convolutional Neural Networks

Sajjad Mozaffari, Eduardo Arnold, Merhdad Dianati,
and Saber Fallah

Abstract—Lane change (LC) is one of the safety-critical manoeuvres in highway driving according to various road accident records. Thus, reliably predicting such manoeuvre in advance is critical for the safe and comfortable operation of automated driving systems. The majority of previous studies rely on detecting a manoeuvre that has been already started, rather than predicting the manoeuvre in advance. Furthermore, most of the previous works do not estimate the key timings of the manoeuvre (e.g., crossing time), which can actually yield more useful information for the decision making in the ego vehicle. To address these shortcomings, this paper proposes a novel multi-task model to simultaneously estimate the likelihood of LC manoeuvres and the time-to-lane-change (TTLC). In both tasks, an attention-based convolutional neural network (CNN) is used as a shared feature extractor from a bird's eye view representation of the driving environment. The spatial attention used in the CNN model improves the feature extraction process by focusing on the most relevant areas of the surrounding environment. In addition, two novel curriculum learning schemes are employed to train the proposed approach. The extensive evaluation and comparative analysis of the proposed method in existing benchmark datasets show that the proposed method outperforms state-of-the-art LC prediction models, particularly considering long-term prediction performance.

Index Terms—Vehicle Behaviour Prediction, Automated Driving, Multi-task Learning, Curriculum Learning, Attention Mechanism

I. INTRODUCTION

ANTICIPATING the future behaviour of surrounding vehicles is a critical function of both Advanced Driving Assistance Systems (ADAS) and fully automated driving systems. Failing to do so may lead to either hazardous driving decisions or forcing unduly conservative driving, compromising the safety or efficiency of the driving system, respectively. In highway driving, lane change (LC) manoeuvres are considered to be safety-critical as they can lead to hazardous interference with the traffic in other lanes. A major crash dataset collected between 2010 and 2017 in the United Arab Emirates indicates that accidents associated with unsafe LC manoeuvres are among the main causes of severe injuries

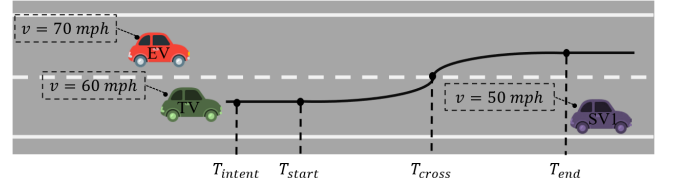


Fig. 1: An example of an LC scenario in a left-hand driving road system.

in highway driving [1]. Although monitoring the indicator signals can be a good detector of LC manoeuvres, studies in USA [2] and China [3] show that less than 50% of drivers are using signal indicators for doing an LC manoeuvre. The LC manoeuvres that occur without proper signalling are often the culprit in accidents. Such hazards can be detected by analysing the motion of the vehicles, which is the main focus of this paper. A reliable LC prediction model in such cases can provide an early warning of emerging LC manoeuvres of other vehicles. Such information can then be used by the ego-driver or the automated driving system to pro-actively make driving decisions and alleviate the risk of accidents associated with LC manoeuvres. An early manoeuvre prediction has a particularly higher value in highway driving scenarios, where the high-speed of vehicles require a more agile driving style and decision making.

An example of an LC scenario in a highway driving environment is illustrated in Figure 1. In this scenario, the Target Vehicle (TV) decides to perform a lane change manoeuvre at time T_{intent} due to the slow-moving preceding vehicle (i.e., SV1: Surrounding Vehicle 1). The LC manoeuvre starts at T_{start} , as the vehicle drifts towards the left lane marking. The TV crosses the lane marking at T_{cross} and finishes its LC manoeuvre by stabilizing its lateral position at the centre of the left lane at T_{end} . The Ego vehicle (EV), which is already driving on the left lane, is supposed to decelerate as soon as it realises the imminent LC manoeuvre by the TV. Therefore, the EV needs to have an early and reliable prediction of the LC manoeuvre and its key timings (e.g., T_{cross}) to perform a smooth and safe deceleration.

There have been several studies on LC prediction in the literature. A major group of existing studies has shown to be able to predict a lane crossing that occurs up to 2.5 seconds in the future [4], [5], while an LC manoeuvre, from T_{start} to

This work was supported by Jaguar Land Rover and the U.K.-EPSRC as part of the jointly funded Towards Autonomy: Smart and Connected Control (TASCC) Programme under Grant EP/N01300X/1

S. Mozaffari, E. Arnold, and M. Dianati are with the Warwick Manufacturing Group, University of Warwick, Coventry CV4 7AL, U.K. (e-mail: sajjad.mozaffari, e.arnold, m.dianati@warwick.ac.uk)

S. Fallah is with the Department of Mechanical Engineering Sciences, University of Surrey, Guildford, GU2 7XH, U.K. (e-mail: s.fallah@surrey.ac.uk)

T_{end} , usually takes between 3 to 5 seconds [6]. This means that most existing studies can only predict an LC manoeuvre after T_{start} , i.e., after the manoeuvre has already started. These studies mostly rely on detecting the lateral drift of the TV towards the lane marking. However, there are fewer clues in the past motion of the TV for predicting its future manoeuvre in longer horizons. Therefore, long-term prediction approaches need to understand the traffic context around the TV, rather than solely analysing the recent motion of the TV. In recent years, some studies attempted to extend the prediction horizon by using deep learning-based models, mainly Long Short-Term Memories (LSTMs) [7], [8]. However, the use of LSTMs for long-term LC prediction is impeded by their shortcoming in extracting spatial interdependency which is required to model the interaction among nearby traffic agents.

In most existing studies [5], [7], [9]–[12] the problem of LC prediction is defined as predicting the likelihood of LC manoeuvres over the next few seconds. In such a formulation, an LC manoeuvre of the TV occurring early in the future is treated equally as an LC manoeuvre happening farther in time. As a result, such an approach cannot inform the EV about the key timings of the TV's manoeuvre, which is crucial for safe and comfortable trajectory planning in automated vehicles.

In this paper, we address the aforementioned shortcomings by proposing a multi-task attention-based prediction model. We apply a novel Convolutional Neural Network (CNN) with spatial attention to a bird's eye view representation of the traffic context around the TV to extract relevant features. An attention module is employed to selectively focus on the most informative areas of the TV's surroundings to improve the feature extraction process. The features extracted by the attention-based CNN are then used to simultaneously predict the likelihood of LC manoeuvre and the time-to-lane-change in a Multi-Task Learning (MTL) approach. Also, two Curriculum Learning (CL) criteria are introduced during the training phase to increase the generalisation of the proposed model. The proposed joint LC and TTLC prediction model is trained and evaluated using a public large scale trajectory dataset collected from German highways [13]. The contributions of this work are summarised below:

- A novel attention-based CNN to extract relevant features for early LC prediction.
- A multi-task learning approach to predict the TTLC in addition to LC manoeuvres likelihood.
- Two novel curriculum learning criteria used during the training phase.
- Comprehensive performance evaluation of the proposed model and comparison with state-of-the-art prediction models.

The rest of this paper is organised as follows. Section II reviews recent LC prediction approaches based on their input representation, prediction model, and output type. Section III discusses the system model and problem formulation. Section IV introduces the proposed method and its key components. Section V presents the experiments' setup for evaluating the performance of the proposed method, key results from those evaluations and the discussions of the insights that can

be learned from our performance evaluation. Finally, some key concluding remarks are given in section VI.

II. RELATED WORKS

A review of vehicle behaviour prediction approaches is provided in [14], in which existing studies are classified into three levels with an increasing degree of abstraction: physics-based, manoeuvre-based, and interaction-aware approaches. Since the publication of this review paper in 2014, several new state-of-the-art (SOTA) prediction approaches, have been proposed. Most of these approaches belong to the most advanced class of prediction model in [14] (i.e., interaction-aware). Our previous survey [15] provides a review of such SOTA studies, which are powered by recent advances in machine learning. In this section, we review the SOTA approaches specifically for LC prediction and highlight how our proposed LC prediction model is differentiated from them. Following [15], our review is categorized based on the input representation, prediction model, and output type of the LC prediction approaches.

A. Input representation

Most of the existing studies utilise a list of hand-crafted features describing the motion of the TV and its surrounding vehicles [7], [8], [10], [11], [16]–[23]. These features include the lateral position in the lane, velocity, acceleration, time-gap, heading angle, relative distance, and so on. Some of these studies also contain features describing the driving environment such as distance to the nearest on- or off-ramp [19] and the existence of the lanes [8], [20]. In addition, in studies where the LC manoeuvre of the EV is predicted, the state of the ego-driver (e.g., head movement, gaze movement, etc.) is often included as an input [24]. However, to keep the generality of our approach in this paper, we do not consider such data since the driver's state of other vehicles are usually unobservable. Selecting a list of hand-crafted features requires the expert's knowledge and might not result in optimal choices for the prediction model. In contrast to hand-crafted feature selection, some of the existing studies utilize Deep Neural Networks (DNNs) to learn relevant features from raw sensor data [5], [9]. Although such a strategy leads to no information loss, large computational resources are required to learn relevant features from high-dimensional raw sensor data, which is challenging due to the limited computational resources of an automated vehicle. Therefore, some studies try to learn features from a simplified bird eye view (BEV) representation of the driving environment instead of raw sensor data. This representation depicts vehicles as their bounding boxes and the road markings. Although the texture information is lost in a simplified BEV representation, it has a significantly lower dimensionality compared to raw sensor data. Providing sufficient training data and enriched BEV representation, the prediction model can learn informative features which were not obvious to domain experts in the first place. In [4], [12], examples of such simplified BEV representation are used for LC prediction. In this paper, we adopt a similar approach and carry out some modifications to improve the feature learning process. Section IV-A explains the details of the simplified BEV representation used in our study.

B. Prediction Model

A group of existing studies utilize graphical models to predict LC manoeuvre. Graphical models are probabilistic models for which a graph, defined using domain knowledge, expresses the conditional dependencies among input, output, and hidden random variables. In [21], a Bayesian network is used to compute the driver's contentedness (i.e., likelihood of occupancy) for all lanes the driver could drive. The driver's contentedness for each lane is then employed to predict the LC intentions. In [20], a hybrid Dynamic Bayesian Network (DBN) is adopted to predict LC intention using a list of interaction-aware features. The latent variables of the prediction model are pre-trained using simulation data, followed by training on German highway driving data. Since exact inference is intractable in DBNs, time-series information is not considered in the inference process. A three-layer DBN has been used in [22] to estimate the driver LC intention and driver characteristic. Then, a Gaussian process is exploited to predict trajectory based on predicted LC manoeuvre. The authors of [22] reported achieving 95% accuracy in LC prediction; however, the prediction horizon for this performance has not been reported. The advantage of graphical models lies in their ability to interpret the model's prediction by examining the values of the graph nodes. However, the drawback of such an approach stems from their limited expression capabilities since no reasoning can be done beyond the fixed relation defined between the graph nodes. In addition, the exact inference in graphical models is often intractable.

Most recent works exploit DNNs for LC prediction. For example, fully connected feed-forward neural networks have been used in [11], [16], [17], [23]. Several existing studies apply variants of recurrent neural networks to predict LC manoeuvre [7], [8], [10], [18], [19], inspired by their success in data sequence analysis. In [10] and [18], a single LSTM is applied to TV-only and interaction-based features for LC prediction, respectively. In [7], a model containing several Gated Recurrent Unit (GRU) is proposed to model pairwise interaction between the TV and each of the SVs. Convolutional Neural Networks (CNNs) have been used in some of the existing studies mainly to model spatio-temporal dependencies in image-like input data such as simplified BEV representation [4], [12], [25] or raw sensor data [5], [9]. In [19], the input features are categorized into TV's motion, Right lane SVs, Left Lane SVs, Same lane SVs and Street features based on which part of the environment they represent. Then, an LSTM is used per feature group to create an internal representation of features. Finally, an attention mechanism is used to specify the importance of each group of features for LC prediction in each data sample. In contrast to most previous studies, in this paper, we use a BEV image representation of the driving environment as input data and adopt a convolutional neural network to learn relevant features from input data. Also, we propose a novel spatial attention mechanism to selectively focus on the important areas of the input representation which enhance the feature learning process.

C. Output Type

The majority of studies on LC prediction formulate the problem as probability estimation of LC manoeuvres, which is considered as a multi-class classification problem. Such a formulation does not allow estimating the time until the occurrence of the LC manoeuvre, which is especially important from the planning perspective of an automated driving system. To deal with this issue, a few studies [8], [24], [26] predict the time when the TV cross the lane marking, known as time-to-lane-change (TTLC). This is because the critical information of a future LC manoeuvre from a safety perspective is the time the vehicle enters another driving lane.

Unlike the existing approaches where either the TTLC or the manoeuvres likelihood is directly estimated, we propose a Multi-Task Learning (MTL) approach to predict both TTLC and manoeuvre likelihood simultaneously within the same model. In machine learning literature, MTL is defined as optimising a neural network for more than one metric [27], [28]. The key idea is to share the hidden representation of the neural network for training multiple downstream tasks in parallel. The training signals of additional tasks serve as inductive bias and yield better generalisation. The inductive bias forces the model to prefer internal representations that can explain more than one task. This is specifically useful when multiple relevant tasks are defined for a model and some of the tasks are more difficult to be learnt on their own. In this case, difficult tasks can *eavesdrop* on the internal representation learnt for easier tasks [27]. MTL has been successful across different applications of machine learning such as natural language processing [29], speech recognition [30], and computer vision [31].

Furthermore, we introduce two novel Curriculum Learning (CL) criteria based on multi-task loss ratio and TTLC to enhance the generalisation of the prediction model. CL is a training strategy that, inspired by learning order in human curricula, starts training of a machine learning algorithm with learning simpler samples and gradually progresses to harder, more difficult samples. This is in contrast to the traditional machine learning training procedure where the model is exposed to all training examples in random order. Introducing curriculum to various applications of machine learning has shown to benefit the speed of convergence and generalization depending on the design of the curriculum and the datasets used [32], [33].

III. SYSTEM MODEL AND PROBLEM DEFINITION

We assume a semi- or fully automated EV aims to predict the lane change manoeuvre of a nearby vehicle, called the TV. Both EV and TV are driving on a straight highway with an arbitrary number of lanes. There is an arbitrary number of surrounding vehicles (SVs) driving in the vicinity of the TV. Similar to most existing studies on LC prediction [4], [7], [10], [11], [16], [19], [22], [25], we assume a BEV camera installed on an infrastructure building or a drone is observing the driving environment, detecting the vehicles, and tracking them while driving on a road section. The vehicles' tracking history, as well as the position of road markings, are assumed to be shared with the EV for the problem of LC prediction.

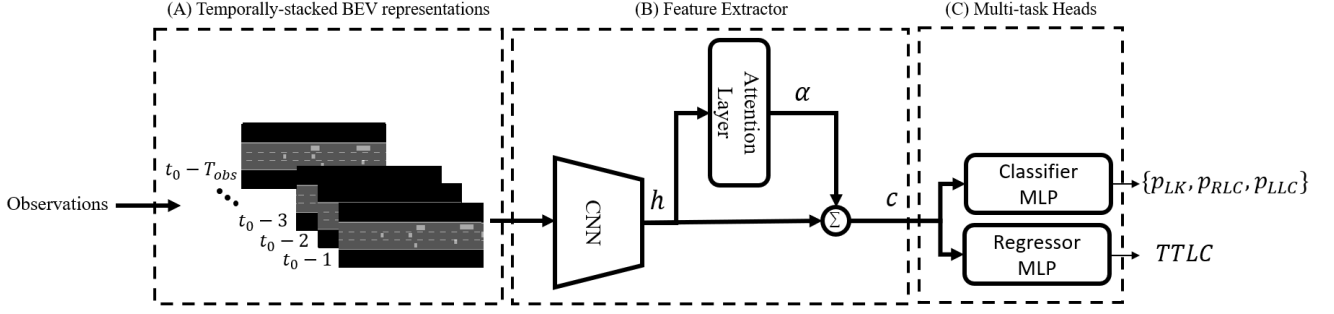


Fig. 2: An overview of key processing steps of the proposed method

We divide the problem of LC prediction into a classification and a regression sub-problem. The classification problem aims to estimate the probability of LC manoeuvres occurring during a prediction window, T_{pw} . The LC manoeuvres are categorized into 1) Right Lane Change (RLC), 2) Left Lane Change (LLC), and 3) Lane Keeping (LK). The value of T_{pw} determines the maximum prediction horizon of the prediction model. In this study, we set $T_{pw} = 5.2\text{sec}$ which enables evaluating the prediction model for long prediction horizons while assures a sufficient number of data samples to be extracted from the selected dataset (refer to section V-A). The regression problem aims to estimate the Time To Lane Change (TTLC). The TTLC is defined as the shortest time until the centre of the TV crosses either left or right lane marking. Predicting TTLC is crucial since it is the first time the TV interferes with the traffic on adjacent lanes. The input data to both subproblems are the TV's and its surrounding vehicles' (SVs) states and the position of lane markings. during a temporal observation window of 2 seconds, $T_{obs} = 2\text{ sec}$.

IV. PROPOSED METHOD

This section presents the proposed multi-task attention-based LC prediction model and the curriculum learning schemes used in the training of the model. The processing steps in the proposed prediction model are summarised as follows:

- (A) The observation of the TV and its SVs during T_{obs} are used to render a simplified BEV representation of the driving environment for each time-step of T_{obs} .
- (B) An attention-based CNN is applied to the temporally stacked BEV representations to extract informative features for LC prediction.
- (C) The features extracted from the previous step are used in two separate fully-connected networks to estimate the probability of LC manoeuvres and the TTLC.

Figure 2 illustrates the proposed method and its key processing steps.

A. BEV Input Data Representation

In this study, the BEV representation is rendered as a single-channel image, as illustrated by some examples in Figure 3. This image is populated by the 2D-bounding boxes, representing the vehicles at a single snapshot of the environment. The

vehicles are considered to be heading horizontally from right to left. The BEV representation also depicts the lane markings and drivable area. Two main characteristics are considered in the BEV representation that facilitates the feature learning process. Firstly, unlike [4], [12] where the image is centred on the EV, we centre the BEV representation on the TV at each time step. This causes the position of lane markings in the representation to indicate the lateral position of the TV in the lane, which is one of the clear predictors of an LC manoeuvre. Centring the representation on the TV also allows encoding the relative states of the SVs compared to the TV which is informative in interaction modelling. Secondly, we use a lateral dimension resolution four times higher than the longitudinal dimension of the representation. This implies a magnification of lateral motions of vehicles in the representation which contains more informative features for the LC prediction problem. The size of the BEV representation in this study is considered to be 200 by 80 pixels covering 200 meters of the road in the longitudinal direction and 20 meters in the lateral direction. The 20 meters lateral coverage assures that the TV's adjacent lanes are always included (see Figure 3). The BEV representation is rendered for all time-steps during the observation window T_{obs} . We stack this representation channel-wise to create a single image with multiple channels each corresponding to one time-step of T_{obs} .

B. Attention-based CNN for Feature Learning

We propose an attention-based CNN to extract relevant spatio-temporal features from the temporally stacked BEV representation. Due to the sparsity of the BEV input representation, it is not required to use a very deep CNN, such as ResNet models [34]. Based on our empirical study, we consider a six-layer CNN including three convolution and three pooling layers. In each convolution layer, 16 learnable convolutional kernels are used with a size of 3×3 . The stride and padding of the kernels are set to 1 so that the size of the representation doesn't change after passing a convolutional layer. Each convolutional layer is followed by a Maximum Pooling (Max-Pool) layer with a size of 2×2 to reduce the dimensionality of input data and a Rectified Linear Unit (ReLU) activation function. Figure 4 illustrates the architecture of the CNN model.

The spatial attention mechanism is proposed to enhance the performance of feature learning. The attention mechanism,

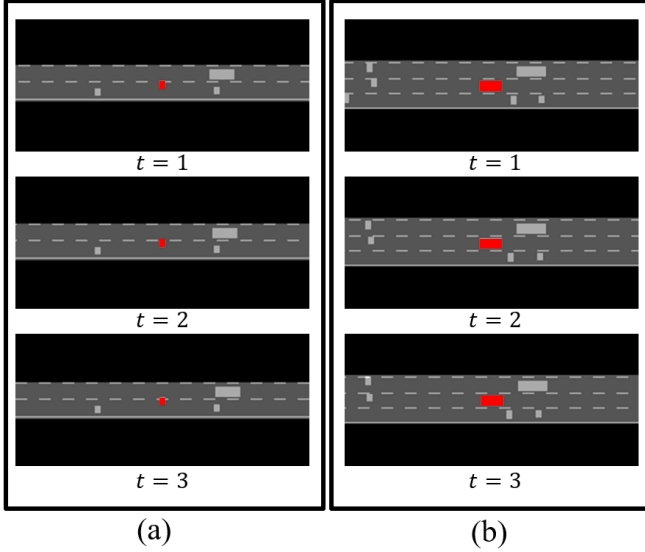


Fig. 3: Two examples of the simplified BEV representation at three different time-steps. Despite the actual position of the TV on side lanes (a), or center lanes (b), it is located at the center of each image. The TV is coloured as red for illustration purposes.

inspired by the human brain, tries to selectively focus on a few relevant parts of the input data to estimate each output. In this study, the goal of employing an attention mechanism is to identify and focus on parts of the environment around the TV that have the most impact on the future behaviour of the TV. In a driving environment, normally only some part of the surrounding vehicles are contributing to the next manoeuvre of a vehicle. For example, a slow-moving vehicle in front usually leads to an RLC if there is a suitable gap in the right lane. In this example, the behaviour of SVs driving on the left lane does not influence the RLC decision made by the TV. Focusing on the relevant areas of the environment around the TV is expected to increase the performance of LC prediction. Therefore, we divide the input representation into four areas, namely, 1) TV's front right, 2) TV's front left, 3) TV's back right, and 4) TV's back left. Since the input images are centred on the TV and vehicles are driving from right to left in input images, these four areas correspond to top-left, bottom-left, top-right, and bottom-right of the input images, respectively. The local connections in convolution and pooling layers of the CNN preserve the spatial location of the extracted features. Hence, the corresponding four areas in the CNN feature map, h are selected as the hidden representations of the respective four areas in the TV's surrounding environment, namely, h_1 to h_4 (see Figure 5). Note that these feature maps represents the TV's surrounding areas for all frames in the observation window. The attention weight for each area is estimated using a linear layer with softmax activation function as follows:

$$\alpha_i = \text{Softmax}(W\hat{h}_i + b), \quad (1)$$

where \hat{h}_i is the flattened vector of h_i . The attention weight for area i is used to create a mask m_i with the same size as h . m_i is filled with values α_i in the regions corresponding to

h_i and zero elsewhere. The output of feature learning model is computed as the context vector c :

$$c = \sum_{i=1}^n m_i h, \quad (2)$$

C. Multi-task Prediction (MTL)

We leverage MTL in training our proposed prediction model for both future LC manoeuvre classification and TTLC regression tasks. Although it is possible to derive the classification information from TTLC estimates [8], we adopt an MTL approach to benefit the generalisation gained by training the model on a similar parallel task. In addition, since the TTLC regression is more difficult than the three-class classification of future LC manoeuvres, the regressor performance can be enhanced by *eavesdropping* on features learnt by the classifier.

Figure 2 provides an overview of the proposed model. The output of the attention-based CNN feature extractor is shared among the classifier and the regressor sub-networks. Each of these sub-networks is a two-layer fully-connected neural network with ReLU activation function and dropout with a ratio of 0.5. The classifier network has 128 hidden neurons with 3 outputs each corresponding to one of the LC manoeuvres. These outputs are followed by a softmax activation function to decode their values as probabilities of LC manoeuvres. The regressor network has 512 hidden neurons with single output that specifies the predicted TTLC. A ReLU activation function is used at the output layer of the regression network as negative values are not accepted for the TTLC. We consider a Cross-Entropy (CE) and Mean-Squared Error (MSE) loss functions for the classifier and regressor sub-networks as below:

$$L_{CE} = -\frac{1}{n} \sum_{i=1}^n \sum_{c=1}^3 y_{i,c} \log \hat{y}_{i,c} \quad (3)$$

$$L_{MSE} = \frac{1}{n} \sum_{i=1}^n (x^i - \hat{x}^i)^2 \quad (4)$$

In the above equations, n is the number of the training samples. $y_{i,c}$ and $\hat{y}_{i,c}$ are the ground truth and predicted probability of sample i belonging to class c , respectively. The ground-truth and predicted TTLC for the sample i are denoted as x^i and \hat{x}^i , respectively. The proposed multi-task model is trained based on the summation of the classifier and regressor losses as below:

$$L = L_{CE} + \gamma L_{MSE} \quad (5)$$

where γ defines the ratio between the regressor and classifier losses.

D. Curriculum Learning (CL)

We utilise curriculum learning based on two criteria specific to the LC prediction problem. First, predicting the LC manoeuvre in samples with smaller TTLC is generally easier compared to samples with larger TTLC. The reason is that as

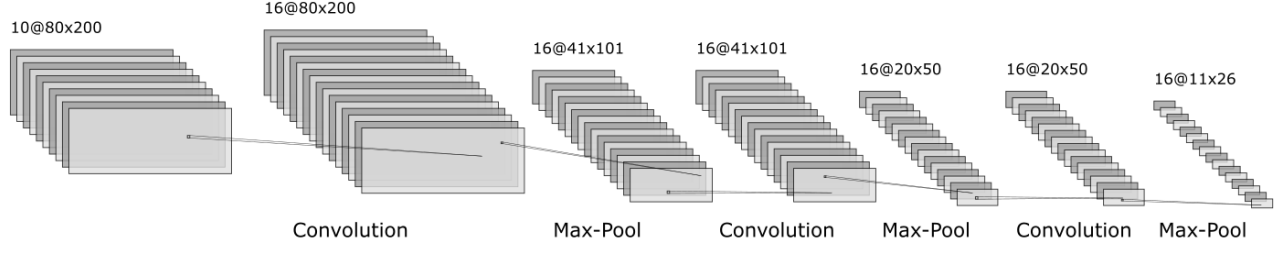


Fig. 4: The architecture of the CNN model.

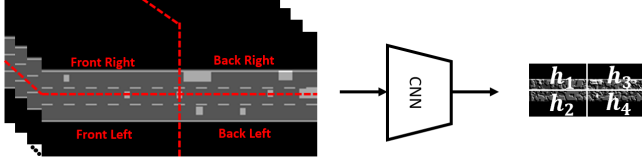


Fig. 5: Four areas of input representation and their corresponding areas in the CNN feature map.

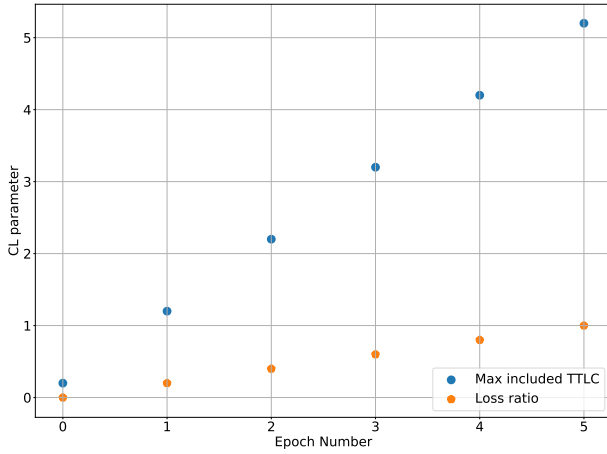


Fig. 6: Values of CL parameters during initial training epochs. Max included TTLC determines the maximum TTLC of included data samples in a epoch.

we get closer to the time when the TV crosses the lane marking, more explicit predictors can be found in the TV's motion. As the TTLC increase, the chance of mistakenly predicting an LC as an LK manoeuvre increases, until $TTLC > T_{pw}$ where the future manoeuvre is actually considered as LK. Therefore, we start training the network with samples with near-zero TTLC and gradually expose samples with larger TTLC to the prediction model. Second, predicting a class within a three-class classification task is normally considered easier than regressing a continuous variable. Hence, we start the training process by giving more importance to the classification task and gradually shift the focus to the regression task. This is achieved by increasing the loss ratio γ in Equation 5 from 0 to 1 during the training phase. Figure 6 shows the TTLC and the loss ratio profile used during the training process.

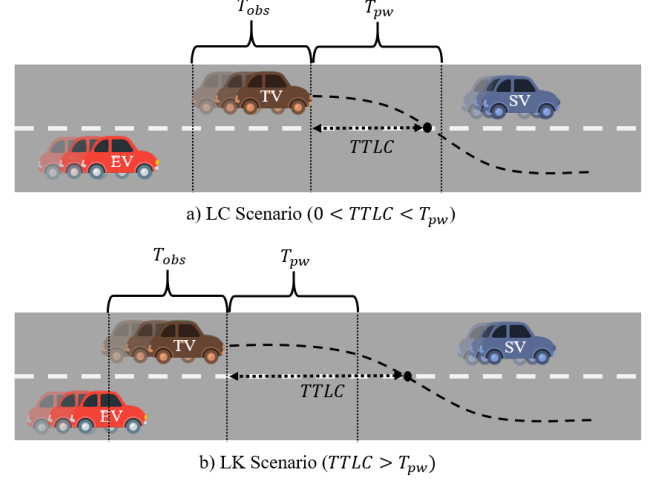


Fig. 7: Examples of (a) RLC and (b) LK scenarios. In LK scenarios, the TV may change its lane after the T_{pw} cut-off.

V. PERFORMANCE EVALUATION

This section describes the evaluation of the proposed LC prediction method. First, the dataset and the LC scenario extraction steps are presented. Then, the implementation details of the proposed method are explained, followed by a discussion of the evaluation metrics. Next, the quantitative results comparing the proposed method with SOTA baseline models and the qualitative results are presented. Finally, an ablation study is performed on key components of our proposed method.

A. Dataset and LC Scenario Extraction

The Highway Drone Dataset (highD) [13] consists of naturalistic vehicle trajectory data recorded at German highways using a drone. It contains the trajectories of 110500 vehicles observed over a highway segment of 420 meters at six different locations. We extract the LC and LK scenarios from the highD dataset to train and evaluate our proposed LC prediction method. An LC scenario is a group of data samples from a single vehicle with TTLC values ranging from 0 to T_{pw} . Each data sample in an LC scenario at a given time t_0 contains the observation of the vehicles' trajectories in the driving environment during $[t_0 - T_{obs}, t_0 - 1]$. To have a balanced number of data samples per each value of TTLC, we do not consider LC scenarios where the corresponding trajectory data is not

TABLE I: Confusion Matrix Used For LC Prediction

Ground-Truth \ Predicted	LK	RLC	LLC
LK	TN*	FP	FP
RLC	FN	TP	FN, FP
LLC	FN	FN, FP	TP

* TN: True Negative, TP: True Positive, FP: False Positive, FN: False Negative

available for the full duration of $T_{obs} + T_{pw}$ sec before the lane crossing. All the samples within an LC scenario are labelled as RLC or LLC according to the direction of the manoeuvre at the end of the scenario. An LK scenario is defined as a group of data samples from a single vehicle with $TTLC > T_{pw}$. Figure 7 illustrates an example of LC and LK scenarios. Similar to LC scenarios, we consider $T_{pw} * FPS$ data samples within an LK scenario. In the highD dataset, the number of LK scenarios are much higher than LC scenarios. However, to keep the dataset balanced, we undersample the LK class so that the number of LK samples is equal to the average between the number of RLC and LLC samples. The challenging LK scenarios for training the prediction model are the ones that the TV changes its lane shortly after T_{pw} , since they can be easily misclassified as LC. Therefore, it is desirable to have more number of such challenging samples. However, there is not a sufficient number of such LK samples in the highD dataset due to the limited length of the covered road section. The highD dataset is published as 60 spreadsheets, from which we select the data in the first 50 files as training data, the next 5 files as validation data, and the remaining 5 files as test data. In total, we have extracted 7487, 932, and 698 LC/LK scenarios from training, validation, and test data, respectively.

B. Implementation Details

We train the proposed model and the re-implemented models from the literature on extracted LC/LK scenarios in the training set of the highD dataset. To train our proposed prediction model, Adam optimiser [35] is used with a learning rate of 0.001 and a maximum of 20 training epochs. The early-stopping technique on validation loss function is used to avoid over-fitting. All the models have been implemented using the PyTorch framework [36] and are trained and evaluated on a single GeForce RTX 2080 Ti GPU. We use a batch size of 64 during the training period. The source code of this study is available at <https://github.com/SajjadMzf/EarlyLCPred>

C. Evaluation Metrics

In this subsection we discuss the metrics we used in evaluation of the future LC classifier and TTLC regressor.

1) *Classification Metrics*: Similar to previous studies, we report accuracy, precision, recall and F1 score over all data samples in the test dataset. However, relying on such metrics is not sufficient for a comprehensive evaluation of a prediction model, especially for applications in automated driving. A reliable LC predictor is expected to have high recall particularly in samples with short TTLC since missing such LC samples

can create safety-related issues for the EV and the surrounding traffic. To this end, we measure the recall (a.k.a. True Positive Rate) of the prediction model with respect to the actual TTLC of the data samples.

Precision, recall, and F1 score are usually defined for a binary classifier. To extend them to a multi-class problem, one can use the "one-vs-all" approach. However, we consider both the RLC and LLC classes as positive classes (similar to [20]), since both are the rarely occurring manoeuvres that we are interested in predicting. Therefore, we consider the confusion matrix for the LC prediction problem as Table I. Note that the data samples with RLC or LLC labels which are classified incorrectly in LLC or RLC classes, respectively, are considered in both FN and FP. The reason is that in such cases the prediction model misses the prediction of the type of LC and generates an incorrect LC alarm.

In addition to having a high recall, an LC prediction model is expected to have a low rate of false LC alarms (False Positive). Although False alarms may not create safety issues, they decrease the comfortability of the driving system because the high rate of false alarms causes frequent, unnecessary slow-downs by the EV. The trade-off between the False Positive Rate (FPR) and True Positive Rate (TPR) of a classifier is reported in terms of the Receiver Operating Characteristic (ROC) Curve and the Area Under the ROC Curve (AUC) of the prediction model.

To measure the average prediction horizon of a prediction model, we report the following two metrics, similar to [23].

- First prediction time, denoted by τ_f : is the time between the first correct prediction of the manoeuvre class and the T_{cross}
- Robust prediction time, denoted by τ_c : is the time between the first moment when the model starts to continuously predict correctly and the T_{cross} .

2) *Regression Metrics*: Although we use the MSE loss function in the training phase, we adopt the RMSE metric to evaluate the performance of the TTLC prediction. The reason is that RMSE is more understandable than MSE since it has the same physical unit as the output data (i.e., seconds). To evaluate the performance of the prediction model for different TTLCs, we use the box plot of the predicted TTLC for each actual TTLC, specifying the median values of the predicted TTLC.

D. Quantitative Results

The results of an LC prediction model depends on the selected dataset and preprocessing steps used for training and evaluation of the model. Factors such as the size of the dataset, the level of noisiness, traffic density, and LC scenario extraction steps can impact the prediction model's results. In addition, parameters of the problem definition can influence the overall performance reported for a prediction model. For example, selecting a smaller prediction window T_{pw} results in better overall prediction performance since it is generally easier to predict manoeuvres with shorter TTLC. To do a fair comparison among our proposed model and the existing solutions, we re-train and evaluate some baseline

TABLE II: Comparison of the proposed LC prediction model with SOTA on HighD dataset

Task	Model	Accuracy	Recall	Precision	F1-score	AUC	τ_f	τ_c	RMSE
Classification	MLP [23]	70.21	67.15	81.43	73.61	72.39	3.89	2.76	-
	LSTM [8]	76.26	70.4	87.78	78.13	80.29	4.19	3.17	-
	CS-LSTM [25]	73.52	78.25	81.02	72.12	76.31	3.92	3.61	-
Regression	LSTM [8]	-	-	-	-	-	-	-	0.999
Dual	Proposed	81.25	85.13	84.68	84.49	87.66	4.79	3.98	0.797

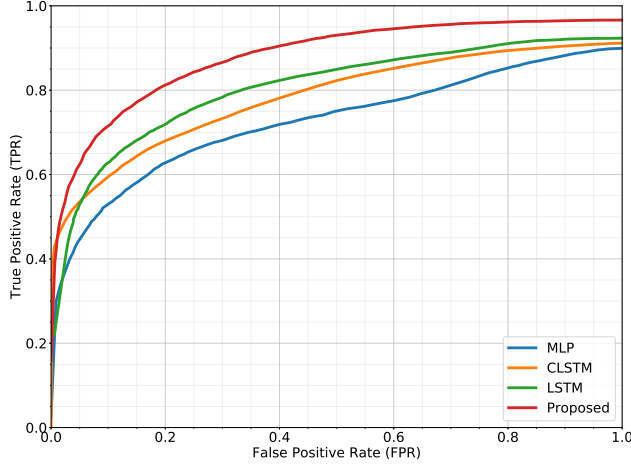
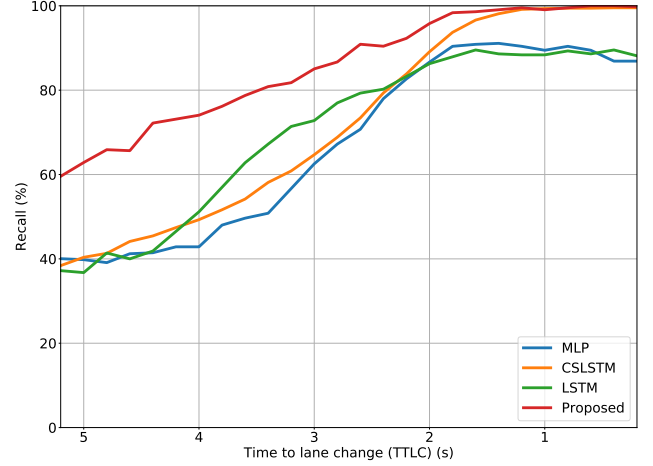
Fig. 8: Receiver Operating Characteristics (ROC) Curve of the proposed method and SOTA on highD dataset with prediction window T_{pw} of 5 seconds.

Fig. 9: Percentages of Recall vs TTLC of the proposed method and SOTA on highD dataset

models from the literature on the same dataset, using the same preprocessing steps and parameters of the problem definition used in this study. We select the following SOTA approaches, where an implementation code or details of implementation are provided:

- **MLP:** Multi-Layer Perceptrons (MLPs) have been used in some existing studies [16], [17], [23]. Here, we re-implement a two-layer MLP with 512 hidden neurons and a ReLU activation function. In [8], [23], a study has been performed on a large-scale dataset to select informative features for MLP and LSTM networks (see Table V in [8]). The study in [8] provides 21 features from which we select 18. The selected features are the ones that are feasible to be extracted from the highD dataset.
- **LSTM:** Several existing studies on LC prediction [7], [8], [19] have used LSTM due to its power in processing data sequences. A single-layer LSTM model is used with a hidden state size of 512 followed by a two-layer fully connected neural network with a hidden state of 128 and 512 for classification and regression tasks, respectively. Similar to the MLP model, we adopt the feature list used in [8].
- **CS-LSTM:** Convolutional social pooling LSTM developed by Deo and Trivedi [25] combines the power of CNNs in spatial interaction modelling with the power of LSTMs in modelling dynamics of each vehicle. The code published by the authors is used to re-train and

evaluate their model with our preprocessed dataset and the parameters used in our problem definition.

Table II shows the results of the selected models for both classification and regression tasks and the results of the proposed model in the dual-task. In the classification task, the proposed model outperforms SOTA approaches with an increase of 4% in accuracy and 6% in F1-score. The LSTM network achieves the second-best performance in classification with 76.26% accuracy and 78.13% F1-score. In regard to the prediction horizon, the CSLSTM model ranks first among selected models from the literature by 3.61 seconds robust prediction time. Nevertheless, the proposed model outperforms CSLSTM by 0.4 seconds in the robust prediction time metric. In the regression task, the proposed model improves the RMSE metric by around 0.2 seconds compared to the LSTM network used in [8].

To evaluate the LC prediction performance at different likelihood thresholds, we plotted the ROC curve in Figure 8. The area under the curve (AUC) is reported in Table II. The proposed method outperforms SOTA by around 7% in AUC and has a higher True Positive Rate (TPR) for different thresholds compared to SOTA. Note that even with 100% False Positive Rate (FPR), none of the models achieves 100% TPR. The reason is that there still might be some samples within the positive classes that are classified in wrong positive classes (i.e., RLC data classified as LLC data and vice versa). As we mentioned earlier such samples are reported as both FP and FN of the prediction model. The proposed model, compared to the reported SOTA models, reduces the number of such

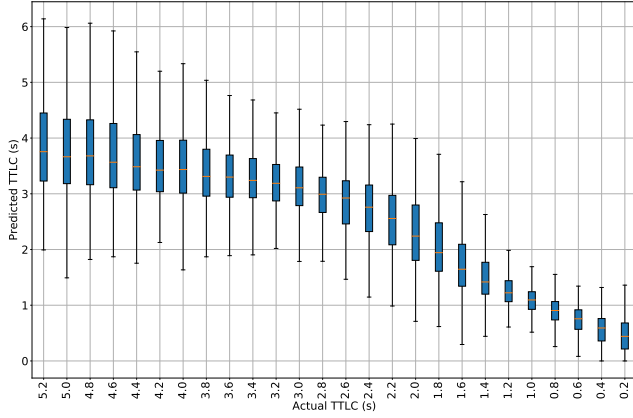


Fig. 10: Box plot of the TTLC predictions on test data of highD

samples by more than half, as indicated in Figure 8.

Figure 9 reports the recall (a.k.a. TPR) vs the TTLC. Both the proposed and the CSLSTM models have close to 100% recall in predictions with TTLC less than 1.5 seconds, while the MLP and LSTM model miss around 10% of LC manoeuvres occurring in less than 1.5 seconds. As discussed previously, any missed short-term predictions can lead to safety-related issues. In terms of long term prediction, the proposed method significantly outperforms the SOTA methods. For instance, in samples with TTLC equals 5.2 seconds, which is the maximum prediction horizon, the proposed method achieves 60% recall which is an improvement of 50% compared to the SOTA models. Note that improving the performance of long-term predictions is challenging because generally there is no explicit change in the TV’s behaviour for LCs that occur far in the future (i.e., more than 3 seconds). Therefore, the prediction model needs to infer the occurrence of an LC by extracting clues from the traffic context around the TV, which makes long-term prediction more challenging.

To evaluate the TTLC regression performance, we report the box plot for all TTLC predictions on the test dataset in Figure 10. The results show that samples with a higher TTLC generate predictions with higher median error and variance. In addition, for TTLC greater than 3.2 seconds the model tends to predict TTLCs less than actual values of TTLC. This can be explained by the fact that samples with TTLC greater than 3 seconds do not exhibit any explicit change in lateral movement of the TV. Therefore, it is not possible to estimate the lane crossing time using the information in lateral speed and distance to lane marking.

E. Qualitative Results

Two examples of RLC and LLC scenarios are represented in Figure 11 and 12. The model’s predictions are illustrated for three values of TTLC, 5, 3, and 1 second. The bottom parts of the images illustrate the four attention zones and their respective weights.

In Figure 11, the TV is going to complete an overtake of a slow-moving truck on the right lane by performing an RLC

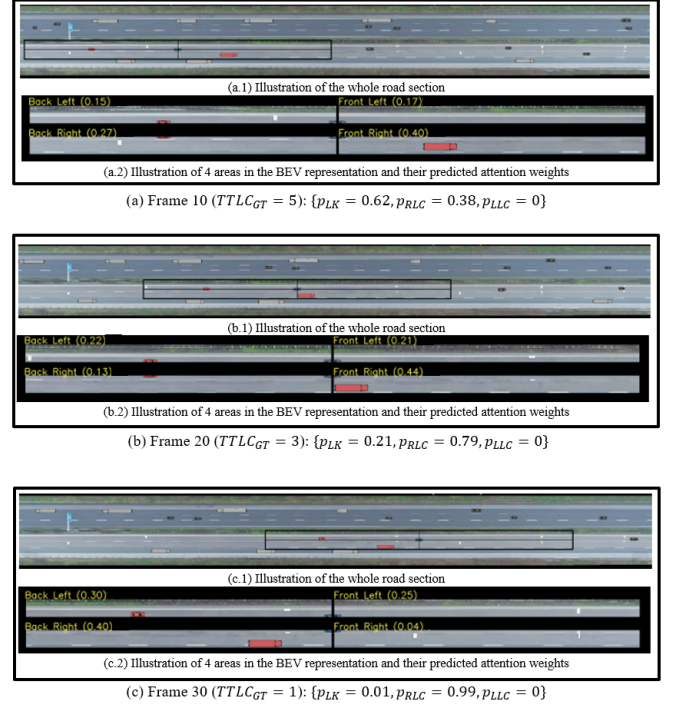


Fig. 11: The prediction model performance in an example of RLC scenario.

manoeuvre. At frame 10, the model predicts a 62% chance for LK in the next 5.2 seconds and a 38% chance for an RLC. At frame 20, the estimated likelihood of an RLC manoeuvre is 79%, even though there is no lateral displacement of the TV up to this frame. The clues of such a manoeuvre can be found in the available gap in the right lane in front of the slow-moving truck. The focus of the attention mechanism shifts from the front-right area to the back-right area in Frame 30, which can be explained by the location of the slow-moving truck.

Figure 12 shows the emerge of an LLC manoeuvre by the TV due to a slow-moving vehicle in front of the TV. In frame 10, the model confidently predicts an LK manoeuvre in the next 5.2 seconds, which could be explained by the absence of a suitable gap in the left lane. At frame 10, the gap starts to appear and a human driver in this scenario may conservatively decide to keep the lane or change its lane in near future. However, the prediction model does not consider the possibility of the second scenario and still predict an LK manoeuvre. Finally, at frame 30, the prediction model estimates the upcoming LLC presumably based on the lateral motion of the TV. The focus of the attention mechanism during these frames are on the traffic on the left lane. We believe this could be explained by the necessity of finding an appropriate gap on the left lane to perform an LLC manoeuvre. The video depicting the model’s qualitative performance in some LK and LC scenarios are found in [37].

F. Ablation Study

In this subsection, we investigate the impact of the key components of the proposed prediction model by evaluating the model performance with different combination of these

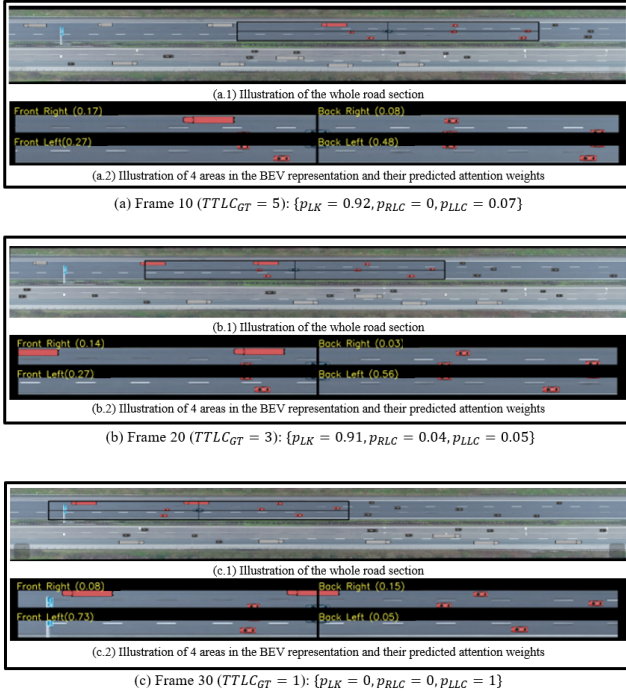


Fig. 12: The prediction model performance in an example of LLC scenario

components. We use the AUC and RMSE on the validation data as evaluation metrics of classification and regression tasks, respectively.

Table III shows the results of the ablation study on Multi-Task Learning (MTL), Attention Mechanism, and Curriculum learning based on MTL loss and TTLC order. In this study, the CNN model (see Figure 4) is used as a baseline and we gradually add the components to investigate their impact in both future LC classification and TTLC regression tasks. The results in Table III shows that using the attention mechanism can enhance the AUC of the classifier by around 3% and slightly decrease the error of the regressor. On the other hand, the MTL when used without attention and curriculum learning, can degrade the performance of the classification task and does not provide improvements for the regression task. However, the MTL is capable of improving the results and achieving the best performance when combined with other key components of the prediction model.

VI. CONCLUSION

This paper proposed a multi-task attention-based CNN model for the early prediction of LC manoeuvres in highway driving scenarios. The prediction model was trained and evaluated using a large-scale naturalistic trajectory dataset. The results shows that the attention-based CNN is capable of extracting interaction-aware features from the surrounding traffic required for long-term prediction. The multi-task approach, boosted by two novel curriculum learning schemes, enables TTLC and manoeuvre likelihood prediction using shared extracted features. Furthermore, the proposed model outperforms selected SOTA LC prediction approaches, demonstrating a

TABLE III: Results of Ablation studies on key components of the proposed method

Task	Attention	CL (Loss)	CL (TTLC)	AUC%	RMSE (s)
C*				88.38	-
R**				-	0.804
MTL				83.11	0.805
MTL	✓			86.89	0.796
MTL	✓		✓	87.79	0.809
MTL	✓	✓		87.97	0.774
MTL	✓	✓	✓	89.43	0.774

* C: Classification, ** R: Regression

reliable short-term prediction and 1.5 times better long-term prediction performances.

In this study, we used a naturalistic trajectory dataset recorded using a drone. Our future research will focus on deploying the proposed approach in an automated driving system. We are specifically interested in identifying the impact of egocentric sensor impairments such as occlusion, sensor noise and limited field of view on vehicle behaviour prediction performance.

REFERENCES

- [1] M. Shawky, "Factors affecting lane change crashes," *IATSS Research*, vol. 44, no. 2, pp. 155 – 161, 2020. [Online]. Available: <http://www.sciencedirect.com/science/article/pii/S0386111219300020>
- [2] E. C. B. Olsen, S. E. Lee, W. W. Wierwille, and M. J. Goodman, "Analysis of distribution, frequency, and duration of naturalistic lane changes," *Proceedings of the Human Factors and Ergonomics Society Annual Meeting*, vol. 46, no. 22, pp. 1789–1793, 2002. [Online]. Available: <https://doi.org/10.1177/154193120204602203>
- [3] R. Dang, F. Zhang, J. Wang, S. Yi, and K. Li, "Analysis of chinese driver's lane change characteristic based on real vehicle tests in highway," in *16th International IEEE Conference on Intelligent Transportation Systems (ITSC 2013)*, 2013, pp. 1917–1922.
- [4] J. Mänttari, J. Folkesson, and E. Ward, "Learning to predict lane changes in highway scenarios using dynamic filters on a generic traffic representation," in *2018 IEEE Intelligent Vehicles Symposium (IV)*, 2018, pp. 1385–1392.
- [5] D. Fernández-Llorca, M. Biparva, R. Izquierdo-Gonzalo, and J. K. Tsotsos, "Two-stream networks for lane-change prediction of surrounding vehicles," in *2020 IEEE 23rd International Conference on Intelligent Transportation Systems (ITSC)*, 2020, pp. 1–6.
- [6] T. Toledo and D. Zohar, "Modeling duration of lane changes," *Transportation Research Record*, vol. 1999, no. 1, pp. 71–78, 2007. [Online]. Available: <https://doi.org/10.3141/1999-08>
- [7] W. Ding, J. Chen, and S. Shen, "Predicting vehicle behaviors over an extended horizon using behavior interaction network," in *2019 International Conference on Robotics and Automation (ICRA)*, 2019, pp. 8634–8640.
- [8] F. Wirthmüller, M. Klimke, J. Schlechtriemen, J. Hipp, and M. Reichert, "Predicting the time until a vehicle changes the lane using lstm-based recurrent neural networks," *IEEE Robotics and Automation Letters*, vol. 6, no. 2, pp. 2357–2364, 2021.
- [9] R. Izquierdo, A. Quintanar, I. Parra, D. Fernández-Llorca, and M. A. Sotelo, "Experimental validation of lane-change intention prediction methodologies based on cnn and lstm," in *2019 IEEE Intelligent Transportation Systems Conference (ITSC)*, 2019, pp. 3657–3662.
- [10] V. Mahajan, C. Katrakazas, and C. Antoniou, "Prediction of lane-changing maneuvers with automatic labeling and deep learning," *Transportation Research Record*, vol. 2674, no. 7, pp. 336–347, 2020. [Online]. Available: <https://doi.org/10.1177/0361198120922210>
- [11] Y. Hu, W. Zhan, and M. Tomizuka, "Probabilistic prediction of vehicle semantic intention and motion," in *2018 IEEE Intelligent Vehicles Symposium (IV)*, 2018, pp. 307–313.

- [12] D. Lee, Y. P. Kwon, S. McMains, and J. K. Hedrick, "Convolution neural network-based lane change intention prediction of surrounding vehicles for acc," in *2017 IEEE 20th International Conference on Intelligent Transportation Systems (ITSC)*, 2017, pp. 1–6.
- [13] R. Krajewski, J. Bock, L. Kloecker, and L. Eckstein, "The highd dataset: A drone dataset of naturalistic vehicle trajectories on german highways for validation of highly automated driving systems," in *2018 21st International Conference on Intelligent Transportation Systems (ITSC)*, 2018, pp. 2118–2125.
- [14] S. Lefèvre, D. Vasquez, and C. Laugier, "A survey on motion prediction and risk assessment for intelligent vehicles," *ROBOMECH Journal*, vol. 1, no. 1, p. 1, Jul 2014. [Online]. Available: <https://doi.org/10.1186/s40648-014-0001-z>
- [15] S. Mozaffari, O. Y. Al-Jarrah, M. Dianati, P. Jennings, and A. Mouzakitis, "Deep learning-based vehicle behavior prediction for autonomous driving applications: A review," *IEEE Transactions on Intelligent Transportation Systems*, pp. 1–15, 2020.
- [16] S. Yoon and D. Kum, "The multilayer perceptron approach to lateral motion prediction of surrounding vehicles for autonomous vehicles," in *2016 IEEE Intelligent Vehicles Symposium (IV)*, 2016, pp. 1307–1312.
- [17] M. Krüger, A. S. Novo, T. Nattermann, and T. Bertram, "Probabilistic lane change prediction using gaussian process neural networks," in *2019 IEEE Intelligent Transportation Systems Conference (ITSC)*, 2019, pp. 3651–3656.
- [18] Q. Zou, Y. Hou, and Z. Wang, "Predicting vehicle lane-changing behavior with awareness of surrounding vehicles using lstm network," in *2019 IEEE 6th International Conference on Cloud Computing and Intelligence Systems (CCIS)*, 2019, pp. 79–83.
- [19] O. Scheel, N. S. Nagaraja, L. Schwarz, N. Navab, and F. Tombari, "Attention-based lane change prediction," in *2019 International Conference on Robotics and Automation (ICRA)*, 2019, pp. 8655–8661.
- [20] T. Rehder, A. Koenig, M. Goehl, L. Louis, and D. Schramm, "Lane change intention awareness for assisted and automated driving on highways," *IEEE Transactions on Intelligent Vehicles*, vol. 4, no. 2, pp. 265–276, 2019.
- [21] T. Rehder, W. Muenst, L. Louis, and D. Schramm, "Learning lane change intentions through lane contentedness estimation from demonstrated driving," in *2016 IEEE 19th International Conference on Intelligent Transportation Systems (ITSC)*, 2016, pp. 893–898.
- [22] J. Liu, Y. Luo, H. Xiong, T. Wang, H. Huang, and Z. Zhong, "An integrated approach to probabilistic vehicle trajectory prediction via driver characteristic and intention estimation," in *2019 IEEE Intelligent Transportation Systems Conference (ITSC)*, 2019, pp. 3526–3532.
- [23] F. Wirthmüller, J. Schlechtriemen, J. Hipp, and M. Reichert, "Teaching vehicles to anticipate: A systematic study on probabilistic behavior prediction using large data sets," *IEEE Transactions on Intelligent Transportation Systems*, pp. 1–16, 2020.
- [24] Z. Yan, K. Yang, Z. Wang, B. Yang, T. Kaizuka, and K. Nakano, "Time to lane change and completion prediction based on gated recurrent unit network," in *2019 IEEE Intelligent Vehicles Symposium (IV)*, 2019, pp. 102–107.
- [25] N. Deo and M. M. Trivedi, "Convolutional social pooling for vehicle trajectory prediction," in *Proceedings of the IEEE Conference on Computer Vision and Pattern Recognition (CVPR) Workshops*, June 2018.
- [26] O. Gallitz, O. De Candido, M. Botsch, R. Melz, and W. Utschick, "Interpretable machine learning structure for an early prediction of lane changes," in *Artificial Neural Networks and Machine Learning – ICANN 2020*, I. Farkas, P. Masulli, and S. Wermter, Eds. Cham: Springer International Publishing, 2020, pp. 337–349.
- [27] R. Caruana, "Multitask learning," *Machine learning*, vol. 28, no. 1, pp. 41–75, 1997.
- [28] S. Ruder, "An overview of multi-task learning in deep neural networks," *CoRR*, vol. abs/1706.05098, 2017. [Online]. Available: <http://arxiv.org/abs/1706.05098>
- [29] R. Collobert and J. Weston, "A unified architecture for natural language processing: Deep neural networks with multitask learning," in *Proceedings of the 25th International Conference on Machine Learning*, ser. ICML '08. New York, NY, USA: Association for Computing Machinery, 2008, p. 160–167. [Online]. Available: <https://doi.org/10.1145/1390156.1390177>
- [30] L. Deng, G. Hinton, and B. Kingsbury, "New types of deep neural network learning for speech recognition and related applications: an overview," in *2013 IEEE International Conference on Acoustics, Speech and Signal Processing*, 2013, pp. 8599–8603.
- [31] R. Girshick, "Fast r-cnn," in *2015 IEEE International Conference on Computer Vision (ICCV)*, 2015, pp. 1440–1448.
- [32] Y. Bengio, J. Louradour, R. Collobert, and J. Weston, "Curriculum learning," in *Proceedings of the 26th Annual International Conference on Machine Learning*, ser. ICML '09. New York, NY, USA: Association for Computing Machinery, 2009, p. 41–48. [Online]. Available: <https://doi.org/10.1145/1553374.1553380>
- [33] X. Wang, Y. Chen, and W. Zhu, "A comprehensive survey on curriculum learning," 2020.
- [34] K. He, X. Zhang, S. Ren, and J. Sun, "Deep residual learning for image recognition," in *Proceedings of the IEEE Conference on Computer Vision and Pattern Recognition (CVPR)*, June 2016.
- [35] D. P. Kingma and J. Ba, "Adam: A method for stochastic optimization," 2017.
- [36] A. Paszke, S. Gross, F. Massa, A. Lerer, J. Bradbury, G. Chanan, T. Killeen, Z. Lin, N. Gimelshein, L. Antiga, A. Desmaison, A. Köpf, E. Yang, Z. DeVito, M. Raison, A. Tejani, S. Chilamkurthy, B. Steiner, L. Fang, J. Bai, and S. Chintala, "Pytorch: An imperative style, high-performance deep learning library," 2019.
- [37] S. Mozaffari, "Earlylcprediction- youtube," https://youtu.be/uFwp8_VDhw, September 2021.

Sajjad Mozaffari is a PhD candidate with the Warwick Manufacturing Group (WMG) at University of Warwick, UK. He recieved the B.Sc. and M.Sc. degrees in Electrical Engineering at the University of Tehran, Iran in 2015 and 2018, respectively. His research interests include machine learning, computer vision, and connected and autonomous vehicles.

Eduardo Arnold Eduardo Arnold is a PhD candidate with the Warwick Manufacturing Group (WMG) at University of Warwick, UK. He completed his B.S. degree in Electrical Engineering at Federal University of Santa Catarina (UFSC), Brazil, in 2017. He was also an exchange student at University of Surrey through the Science without Borders program in 2014. His research interests include machine learning, computer vision, connected and autonomous vehicles. He is currently working on perception for autonomous driving applications at the Intelligent Vehicles group within WMG.

Mehrdad Dianati Professor Mehrdad Dianati is the Head of Intelligent Vehicles Research Department and the Technical Research Lead in the area of Networked Intelligent Systems at the Warwick Manufacturing Group (WMG), the University of Warwick, UK. The focus of his research is on the application of Digital Technologies (Information and Communication Technologies and Artificial Intelligent) for the development of future mobility and transport systems. He has over 29 years of combined industrial and academic experience, with 20 years in various leadership roles in multi-disciplinary collaborative R&D projects. He works closely with the Automotive and ICT industries as the primary application domains of his research. He is also the Director of Warwick's Centre for Doctoral Training on Future Mobility Technologies, training doctoral researchers in the areas of intelligent and electrified mobility systems in collaboration with the experts in the field of electrification from the Department of Engineering of the University of Warwick. In the past, he has served as an Editor for the IEEE Transactions on Vehicular Technology and several other international journals, including IET Communications. Currently, he is the Field Chief Editor of Frontiers in Future Transportation.

Saber Fallah Dr Saber Fallah is the Director of the Connected Autonomous Vehicles Lab (CAV-Lab) at the Department of Mechanical Engineering Sciences at the University of Surrey, where he leads several research activities funded by the UK and European governments (e.g. EPSRC, Innovate UK, H2020, KTP) in collaboration with major companies active in autonomous vehicle and robot technologies. CAV-Lab provides a unique laboratory to design, develop and test the next generation of robotics and autonomous systems used for remote assembly and manufacture, highly automated transportation systems and missions in hazardous environments including space. CAV-Lab also provides expertise in distributed control systems, AI and machine learning, and predictive optimisation techniques. Prior to joining the University of Surrey, he was part of a cross-disciplinary team in Green Intelligent Transportation Systems research (University of Waterloo, Canada). His research interests include reinforced deep learning, advanced control and prediction and their application to autonomous robot systems.